MECHANIKA TEORETYCZNA
I STOSOWANA
Journal of Theoretical
and Applied Mechanics
2, 35, 1997

INSTABILITY OF NON-PARALLEL COMPRESSIBLE BOUNDARY LAYER

EWA TULISZKA-SZNITKO

Institute of Thermal Engineering, Technical University of Poznań
e-mail: sznitko@orion.put.edu.pl

Linear compressible stability of non-parallel boundary layer is studied using the parabolized stability theory. Evolution of disturbances in a hypersonic flow around a sharp cone of zero angle of attack is studied for freestream Mach number 8.0. The parabolized stability equations are solved using the backward second order finite difference scheme in a streamwise direction, and fourth order two point scheme in a wall-normal direction. The influence of nonparallelizm on the first and second mode disturbances, respectively, is analysed.

Key words: laminar-turbulent transition, instability

1. Introduction

The increasing cost of petrolium products and their reduced availability in future impose new requirements of the design process of airplanes and rockets. The phenomenon of transition from laminar to turbulent flow becomes of primary importance when the design of airplanes or rockets is considered. A laminar flow is desired over the surface for two reasons: low skin friction drag and low surface heating at a hypersonic speed. To predict the heat transfer and skin friction along the surface of a body exposed to the flow field, the region where the transition from laminar to turbulent flow takes place has to be determined. Till now the transition prediction methods have been based on a semi-empirical method using the linear parallel stability theory (local theory), or on direct numerical methods. In the linear parallel approach the Navier-Stokes equations are reduced to ordinary differential equations which along with the homogeneous boundary conditions constitute an eigenvalue problem. This method is strongly simplified nevertheless numerically very

efficient. On the other hand, the direct numerical simulation, which yields full description of the flow in the transition region, is computationally very expensive and is still used only for simple model flows. Govering the need for more accurate calculations than those caused on the local theory and less expensive than using the direct methods (cf Bertolotti (1991), Bertolotti et al. (1992)) introduced the parabolized stability theory. In the parabolized stability theory the local growth of disturbance is influenced by local flow conditions and upstream spatial amplification whereas in the local stability theory the local growth is influenced only by local flow conditions. In globally unstable flows the entire flow field influences the local disturbances. In the parabolized stability theory the effect of boundary layer growth and other history effects associated with initial conditions can be properly accounted for. It is computationally a very effective model for analysis of instability of two and three dimensional flows.

The parabolized stability equations are obtained by parabolization of equations of disturbances. The parabolic nature of resulting system of equations limits, however, the applicability of the approach to convectivelly unstable flows, in which the upstream propagation of disturbances is negligible.

The parabolized stability method can be used for linear and nonlinear parts of laminar-turbulent transition region. The nonlinear results of Bertolotti (1991), Bertolotti et al. (1992) showed close agreement with the results obtained using direct methods.

The effect of boundary layer growth on the stability characteristics of compressible flow was studied by El-Hady (1991), (1981), Gapanov (1981) who used multiple scales method and by Bertolotti (1991), Chang et al. (1991), (1993), Dallmann (1993), Simen et al. (1994) who used the parabolized stability theory. From these results we know that in supersonic flow the influence of nonparallelizm is stronger on the three dimensional first mode than on the two dimensional second one.

In the present paper a parabolized stability method is described and used to study the transition region in hypersonic flow around a sharp cone of zero angle of attack. The solutions are compared to the experimental data of Stetson (1983) and numerical results of Dallman (1993). The effect of nonparallelizm and the influence of viscous-inviscid interaction between shock wave and boundary layer are tested. Calculations are made to explain discrepancies between the experimental results of Stetson and calculated amplification rates of disturbances.

In sections 2, 3 and 4 a general description of the parabolized theory formulation and numerical procedure used to solve the governing equations are shown. The results are presented and discussed in sections 5 and 6.

2. Formulation of the problem

The parabolized stability equations are derived from the Navier-Stokes equations, energy equation and continuity equation of a viscous compressible gas

$$\frac{\partial \rho}{\partial t} + \nabla \cdot (\rho \boldsymbol{V}) = 0$$

$$\rho\Big(\frac{\partial \boldsymbol{V}}{\partial t} + (\boldsymbol{V} \cdot \nabla)\boldsymbol{V}\Big) = -\nabla p - \nabla \times [\mu(\nabla \times \boldsymbol{V})] + \nabla[(\lambda + 2\mu)\nabla \cdot \boldsymbol{V}] \quad (2.1)$$

$$\rho c_p\Big(\frac{\partial \tau}{\partial t} + (\boldsymbol{V} \cdot \nabla)\tau\Big) = \nabla \cdot (k\nabla\tau) + \frac{\partial \rho}{\partial t} + (\boldsymbol{V} \cdot \nabla)p + \Phi$$

where

$\boldsymbol{V}$	–	velocity vector
ρ	–	density
τ	–	temperature
μ, λ	–	first and second viscosity, respectively
c_p	–	specific heat at a constant pressure
t	–	time
p	–	pressure
k	–	coefficient of thermal conductivity.

The dissipation function Φ is

$$\Phi = \lambda(\nabla \cdot \boldsymbol{V})^2 + \frac{\mu}{2}(\nabla \boldsymbol{V} + \nabla \boldsymbol{V}^{\mathsf{T}})^2 \quad (2.2)$$

The gas is assumed to be perfect so the equation of state is

$$p = T\tilde{R}\rho \quad (2.3)$$

In this research we formulate the compressible stability problem in the body oriented coordinate system (ξ, ζ, η) shown in Fig.1 (ξ, ζ, η are coordinates in the streamwise, wall-normal and spanwise directions, respectively). All lengths are scaled by the viscous scale $\sqrt{\nu_e \xi / U_e}$, velocity by U_e, density by ρ_e, pressure by $\rho_e U_e^2$, time by $\sqrt{\nu_e \xi / U_e}/U_e$ and all other variables by the corresponding boundary layer edge values. Perturbation equations are obtained by decomposing all parameters into there of the steady basic flow $(U, V, W, \tau, \rho_0, k, \mu_0, \lambda_0)$ and the unsteady disturbance flow component parameters $(u', v', w', \tau', \rho', k', \mu', \lambda')$, respectively.

$$\begin{aligned} &u = U + u' \quad && v = V + v' \quad && w = W + w' \quad && \tau = T + \tau' \\ &\rho = \rho_0 + \rho' \quad && k = K + k' \quad && \mu = \mu_0 + \mu' \quad && \lambda = \lambda_0 + \lambda' \end{aligned} \quad (2.4)$$

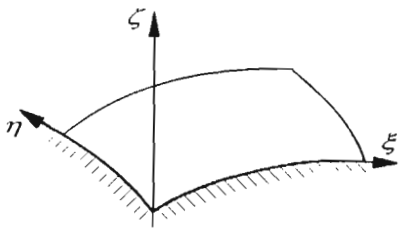

Fig. 1. Schematic picture of the body-oriented coordinate system

where u, v, w are the velocity components in ξ, ζ, η directions, respectively. The ratio of second viscosity to first viscosity is set to

$$\frac{\lambda}{\mu} = \frac{2}{3}(d-1) \tag{2.5}$$

where $d = 0$ represents the Stokes hypothesis which is true for the monoatomic gases. For the polyatomic gases like air $d = 1.2$. In the described algorithm it is assumed that the ratio of specific heat is constant

$$\chi = \frac{c_p}{c_v} = 1.4 \tag{2.6}$$

The Prandtl number is also constant

$$\mathrm{Pr} = \frac{c_p \lambda}{\mu} = 0.72 \tag{2.7}$$

The first viscosity is calculated using the Sutherland law. The fluctuations of thermal conductance and first and second viscosity are written as a first order expansion in temperature

$$\mu' = \frac{\partial \mu_0}{\partial T}\tau' \qquad \lambda' = \frac{\partial \lambda_0}{\partial T}\tau' \qquad k' = \frac{\partial K}{\partial T}\tau' \tag{2.8}$$

Substituting Eqs (2.3) $\div$ (2.8) into Eqs (2.1) and subtracting the equations corresponding to the steady basic state, we obtain the governing equations for the disturbances

$$\begin{aligned} \mathbf{F}\frac{\partial \boldsymbol{\Psi}}{\partial t} + \mathbf{A}\frac{\partial \boldsymbol{\Psi}}{\partial \zeta} + \mathbf{B}\frac{\partial \boldsymbol{\Psi}}{\partial \xi} + \mathbf{C}\frac{\partial \boldsymbol{\Psi}}{\partial \eta} + \mathbf{D}\boldsymbol{\Psi} = \mathbf{H}_{\xi\xi}\frac{\partial^2 \boldsymbol{\Psi}}{\partial \xi^2} + \mathbf{H}_{\xi\zeta}\frac{\partial^2 \boldsymbol{\Psi}}{\partial \xi \partial \zeta} + \\ + \mathbf{H}_{\zeta\zeta}\frac{\partial^2 \boldsymbol{\Psi}}{\partial \zeta^2} + \mathbf{H}_{\eta\xi}\frac{\partial^2 \boldsymbol{\Psi}}{\partial \eta \partial \xi} + \mathbf{H}_{\zeta\eta}\frac{\partial^2 \boldsymbol{\Psi}}{\partial \zeta \partial \eta} + \mathbf{H}_{\eta\eta}\frac{\partial^2 \boldsymbol{\Psi}}{\partial \eta^2} \end{aligned} \tag{2.9}$$

where $\boldsymbol{\Psi}$ is an unknown vector $\boldsymbol{\Psi} = [u', v', w', p', \tau']^{\mathsf{T}}$ and $\mathbf{F}$, $\mathbf{A}$, $\mathbf{B}$, $\mathbf{C}$, $\mathbf{D}$, $\mathbf{H}$ $(i, j = 1, 3)$ are 5×5 matrices. In the present paper calculations are made for a hypersonic flow around axisymmetric object geometry. The function describing the development of disturbance in a non-parallel flow around the cone of zero angle of attack is given by

$$\boldsymbol{\Psi}(\xi, \zeta, \eta) = \overline{\boldsymbol{\Psi}}(\xi, \zeta) \exp\Big[\mathrm{i}\Big(\int_{\xi_0}^{\xi} \alpha(\xi)\, d\xi + \beta\eta - \omega t\Big)\Big] \tag{2.10}$$

where

$\overline{\boldsymbol{\Psi}}(\xi, \zeta)$ – complex amplitude function, $\overline{\boldsymbol{\Psi}} = [\overline{u}, \overline{v}, \overline{w}, \overline{p}, \overline{\tau}]^{\mathsf{T}}$

α, β – components of the wave number vector in the streamwise and spanwise directions, respectively

ω – frequency.

In the parabolized stability theory we assume that the wave number and flow profiles change slowly in the streamwise direction so there exist the values of α and $\overline{\boldsymbol{\Psi}}$ for which the second derivatives $\partial^2/\partial\xi^2$ and products of the first derivatives of these quantities are negligible. In the region of linear development of disturbances the amplitudes are assumed to be small enough to neglect the nonlinear interaction of the waves with different frequency and spanwise wave number. A great advantage of the parabolized stability theory is the possibility of nonlinear effects to be incorporated. For the nonlinear region of laminar turbulent transition, we assume that the total disturbance can be expressed by the Fourier series

$$\boldsymbol{\Psi} = \sum_{n=-\infty}^{\infty} \sum_{m=-\infty}^{\infty} \overline{\boldsymbol{\Psi}}_{m,n}(\xi, \zeta) \exp\Big[\mathrm{i}\Big(\int_{\xi_0}^{\xi} \alpha_{m,n}(\xi)\, d\xi + n\beta\eta - m\omega t\Big)\Big] \tag{2.11}$$

where $\overline{\boldsymbol{\Psi}}_{m,n}$ and $\alpha_{m,n}$ are the Fourier components of amplitude function and streamwise wave number, respectively.

In this paper we restrict ourselves to the linear part of transition region. Substituting Eqs (2.10) into Eq (2.9) and neglecting the nonlinear terms, we obtain the following system of equations

$$\tilde{\mathbf{A}}\frac{\partial\overline{\boldsymbol{\Psi}}}{\partial\zeta} + \tilde{\mathbf{B}}\frac{\partial\overline{\boldsymbol{\Psi}}}{\partial\xi} + \tilde{\mathbf{D}}\overline{\boldsymbol{\Psi}} = \mathbf{H}_{\xi\xi}\frac{\partial^2\overline{\boldsymbol{\Psi}}}{\partial\xi^2} + \mathbf{H}_{\xi\zeta}\frac{\partial^2\overline{\boldsymbol{\Psi}}}{\partial\xi\partial\zeta} + \mathbf{H}_{\zeta\zeta}\frac{\partial^2\overline{\boldsymbol{\Psi}}}{\partial\zeta^2} \tag{2.12}$$

To solve above elliptic system of equation we must know the outflow boundary condition which is very difficult to predict. However, with appropriate simplification the equations can be parabolized. There are some ways of parabolizing

the governing equations (2.12). For example, Dallmann (1993) introduced the ratio of characteristic lengths of the boundary layer flow in the wall-normal and wall-tangential directions, respectively

$$\frac{\sqrt{\xi \nu_e / U_e}}{\xi} = \frac{1}{\mathrm{Re}} \tag{2.13}$$

Dallmann scaled the basic and disturbance flow quantities as well as coordinates in the following powers of the Reynolds number to suppress upstream influence which introduces an elliptic character in governing equations

$$\begin{array}{llll} U = U_T & V = V_T/\mathrm{Re} & W = W_T & T = T_T \\ u' = u'_T & w' = w'_T & v' = v'_T & \\ p = p'_T/\mathrm{Re}^2 & \xi = \xi_T \mathrm{Re} & \zeta = \zeta_T & \eta = \eta_T \end{array} \tag{2.14}$$

where $(\cdot)_T$ denotes transformation.

Following Dallmann in the present paper the flow parameters and coordinates are scaled as in Eqs (2.14). We introduce Eqs (2.14) to the governing equations (2.12) and neglect all terms of order $O(1/\mathrm{Re}^2)$. After back transformation we obtain the equations of parabolized stability theory

$$\tilde{\mathbf{D}}\overline{\boldsymbol{\Psi}} + \tilde{\mathbf{A}}\frac{\partial \overline{\boldsymbol{\Psi}}}{\partial \xi} + \tilde{\mathbf{B}}\frac{\partial \overline{\boldsymbol{\Psi}}}{\partial \zeta} = \mathbf{H}_{\zeta\zeta}\frac{\partial^2 \overline{\boldsymbol{\Psi}}}{\partial \zeta^2} \tag{2.15}$$

With the scaling of pressure introduced in Eqs (2.14) the system of equations (2.15) is of the eighth order in wall-normal direction. However, this system is not completely parabolic. Some terms remain which still allow the upstream propagation of disturbances. As a consequence, there is not only the upper limit for a step size in the streamwise direction but also the lower limit. If the step size is too small the solution procedure will be unstable. Fig.2 shows the instability characteristics $-\alpha_i$ versus the Reynolds number obtained for the flow around a sharp cone for different step sizes $\Delta\xi = 1,\ 3,\ 4,\ 9$, $\beta = 0$, $F = \omega/\mathrm{Re} = 126 \cdot 10^{-6}$, $\mathrm{Ma} = 8.0$). We see that for $\Delta\xi = 1$ and 3 the procedure is unstable.

For the wave approximation (2.10) the amplitude function $\overline{\boldsymbol{\Psi}}$ and wave number α depend on the streamwise coordinate ξ. This results in a kind of ambiguity which can be removed by using the so-called normalization condition (cf Bertolotti (1991)). The normalization condition requires the selected amplitude function in the defined position to be constant. In the present paper we have chosen the amplitude of the velocity component perpendicular to the wall

$$\overline{v}(\zeta_n) = \mathrm{const} \tag{2.16}$$

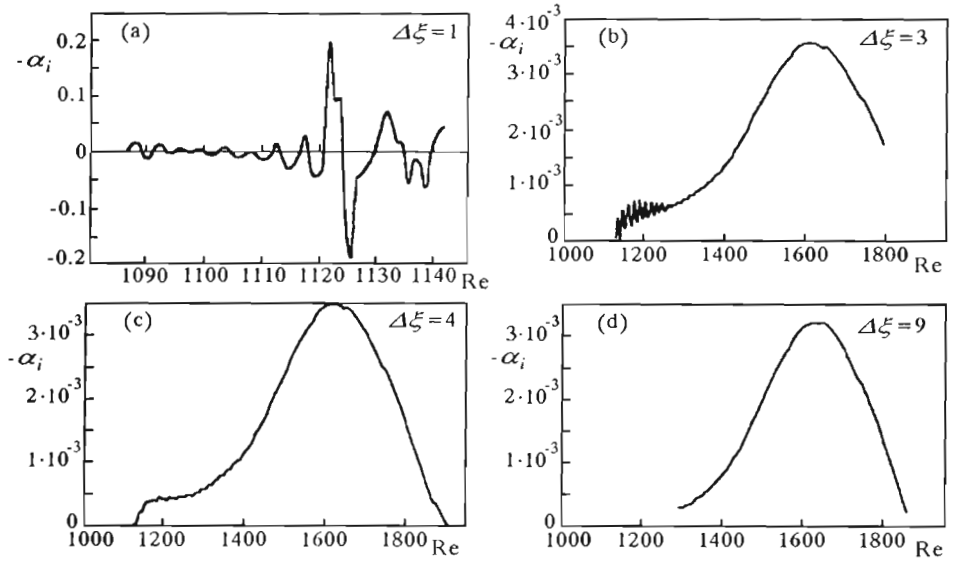

Fig. 2. Instability characteristics of second mode obtained from the parabolized stability theory for different step sizes $\Delta\xi = 1$ (a), 3 (b), 4 (c), 9 (d)

The choice of amplitude and position ζ_n exerts a negligible influence on the instability characteristics. The normalization condition must be satisfied iteratively in every section of the domain (we iterate on α to satisfy Eq (2.16)). The non-local wave number at a given location ξ_1 is given by

$$\alpha_N = \alpha_1 - \mathrm{i}\left(\frac{\partial\overline{\Psi}/\partial\xi}{\overline{\Psi}}\right)_1 \tag{2.17}$$

where α_1 is the local wave number at the considered location obtained as a result of the iteration procedure. The real part of the non-local wave number α_N represents the phase change while the imaginary part is the amplification rate of disturbances. To calculate α_N we must select one dependent variable. Following Chang et al. (1991), in order to calculate the non-local wave number we use the amplitude of velocity component in the streamwise direction at the point where $\overline{u}$ reaches its local maximum.

We have the following homogeneous boundary conditions at the wall and at infinity for the velocity components and temperature amplitude functions

$$\begin{aligned} &\overline{u}(0) = \overline{v}(0) = \overline{w}(0) = \overline{\tau}(0) = 0 \\ &\overline{u}(\zeta) = \overline{v}(\zeta) = \overline{w}(\zeta) = \overline{\tau}(\zeta) = 0 \end{aligned} \tag{2.18}$$

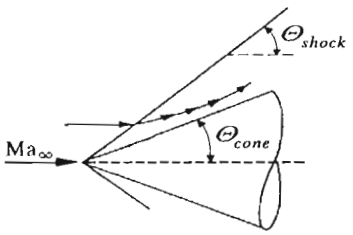

Fig. 3. Schematic picture of sharp cone and oblique shock wave

The above boundary conditions can be replaced by the linearized Rankine-Hugoniot conditions at the shock in a supersonic flow. These linearized conditions represent unsteady motion of the shock due to small disturbances. Chang et al. (1990) showed that introduction of the shock boundary conditions exerts a strong influence on stability of results only when the shock is located near the boundary layer (not far from the tip of cone – Fig.3). As the distance from the tip increases, the shock is located futher from the boundary layer edge and there is no effect of shock boundary conditions on the instability characteristics. In the present paper the calculations are made far from the tip so Eqs (18) are used as the boundary conditions.

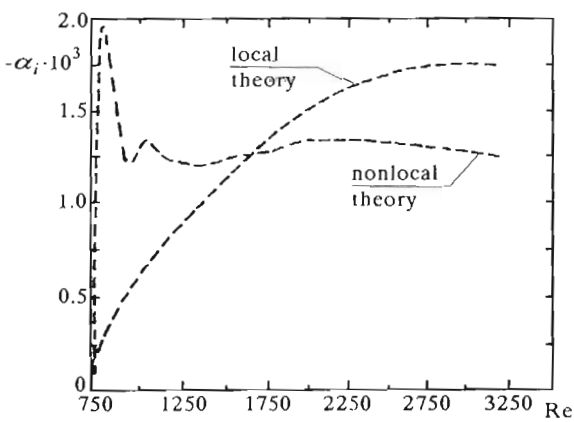

Fig. 4. Transient nonlocal amplification rates of first mode obtained by Dallmann (1993) for $F = 29.5 \cdot 10^{-6}$, $\gamma = 55$

Solving the governing equations (2.15) requires an initial condition. The initial condition should take into account the freestream disturbances which initiate the instability waves in the boundary layer. The initial condition

formulated in this way (which involves the receptivity problem) is not the matter consideration in this paper. We use the solution obtained using the local linear stability theory in the section below the lower branch of the neutral curve (cf Chang et al. (1991)). Solution at this location is precise enough to be used as the initial condition. Sensitivity of the stability characteristics to accuracy of the initial condition was tested, e.g., by Bertolotti (1991) and Dallmann (1993). It was found that the parabolized stability method yields a proper solution provided the initial conditions do not depart too much from the correct solution of linear local theory. However, any imperfection in the initial conditions results in "transients" in the marching solution (Fig.4, Dallmann (1991)).

3. Basic state

For stability analysis we have used a highly accurate solution of the thin layer Navier-Stokes equations as a basic state. Solution of the thin layer Navier-Stokes equations (cf Müller (1991)) was made us accessible by Deutsche Forschungsanstalt für Luft-und Raumfahrt (DLR) in Göttingen. This basic state was used to test the influence of viscous-inviscid interaction between the viscous boundary layer flow and the inviscid shock flow on instability characteristics. If the basic state results from the boundary layer equations using Mangler's transformation (cf Illingworth (1953), Balacumar and Reed (1989), Tuliszka-Sznitko (1993)) the effect of viscous-inviscid interaction is neglected. Fig.5a shows the comparison between the experimental results of Stetson (1983) and the numerical results obtained from the local stability theory for two basic states based on the boundary layer (Tuliszka-Sznitko (1996)) and thin layer Navier-Stokes equations, respectively. We analysed the growth rates α_i versus the disturbance frequencies $F = \omega/\mathrm{Re}$ at a the fixed Reynolds number. Calculations were made for: sharp cone of zero angle of attack, $\mathrm{Re} = 1733$, freestream Mach number 8.0, half-angle 7 degrees cone. We see that more precise modeling of the basic state (including viscous-inviscid interaction) exerts a strong uniformly stabilizing influence on amplified 2D second mode disturbances (wave angle $\gamma = \tan^{-1}\frac{\beta}{\alpha\mathrm{Re}} = 0.0$). With a properly modeled basic state the calculated amplification rates of second mode are in far better agreement with Stetson's experimental data. In the first mode region calculations were made for the most unstable wave angle $\gamma = 30 \div 70$ (for the basic state from the boundary equations) and for the wave angle $\gamma = 55$ for the basic state obtained from the thin layer Navier-Stokes equations. The same

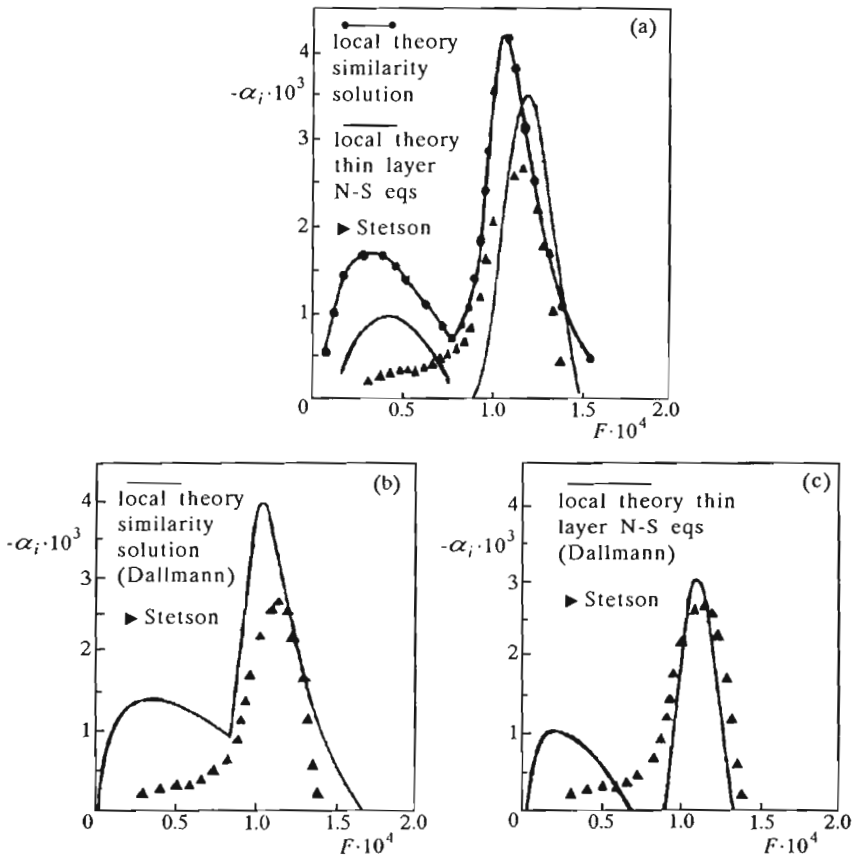

Fig. 5. Effect of viscous-inviscid interaction on the local amplification rate; (a) – results obtained in the present paper for similarity basic state and for basic state from thin layer Navier-Stokes equations, (b) – results obtained for similarity basic state of Dallmann (1993), (c) – results obtained by Dallman for the basic state resulting from the thin layer Navier-Stokes equations

comparison made by Dallmann (1993) is shown in Fig.5b and Fig.5c where the results obtained for the basic state resulting from the boundary equations and thin layer Navier-Stokes equations are shown, respectively. The instability characteristics in Fig.5b and Fig.5c in the first mode region are obtained for the most unstable waves. From Fig.5 we see that relatively good agreement between theory and experiment is reached in the second mode region if the viscous-inviscid interaction is taken into account. Discrepancies in the first mode region are still large.

4. Numerical formulation

Numerical solution of the parabolized stability equations (2.15) requires discretization in ξ and ζ directions. In streamwise direction the second order backward difference scheme is used

$$\frac{\partial \overline{\boldsymbol{\Psi}}}{\partial \xi} = \frac{3\overline{\boldsymbol{\Psi}}_{i,k} - 4\overline{\boldsymbol{\Psi}}_{i-1,k} + \overline{\boldsymbol{\Psi}}_{i-2,k}}{2\Delta\xi} \tag{4.1}$$

For the first step the first order backward scheme is employed

$$\frac{\partial \overline{\boldsymbol{\Psi}}}{\partial \xi} = \frac{\overline{\boldsymbol{\Psi}}_{i,k} - \overline{\boldsymbol{\Psi}}_{i-1,k}}{2\Delta\xi} \tag{4.2}$$

where i and k denote the grid indexes along ξ and ζ, respectively. After discretization in ξ direction we obtain

$$\left[\tilde{\mathbf{D}} + \frac{3}{2\Delta\xi}\tilde{\mathbf{B}}\frac{\partial}{\partial\zeta} - \mathbf{H}_{\zeta\zeta}\frac{\partial^2}{\partial\zeta^2}\right]_{i,k}\overline{\boldsymbol{\Psi}}_{i,k} = \tilde{\mathbf{A}}\frac{4\overline{\boldsymbol{\Psi}}_{i-1,k} - \overline{\boldsymbol{\Psi}}_{i-2,k}}{2\Delta\xi} \tag{4.3}$$

To discretize the above equations in ζ direction, the fourth order accurate two point scheme is used

$$\boldsymbol{\varphi}^k - \boldsymbol{\varphi}^{k-1} = \frac{h_k}{2}\left(\frac{d\boldsymbol{\varphi}^k}{d\zeta} + \frac{d^2\boldsymbol{\varphi}^{k-1}}{d\zeta^2}\right) - \frac{h_k^2}{12}\left(\frac{d^2\boldsymbol{\varphi}^k}{d\zeta^2} - \frac{d^2\boldsymbol{\varphi}^{k-1}}{d\zeta^2}\right) + O(h_k^5) \tag{4.4}$$

where $\boldsymbol{\varphi}^k = \boldsymbol{\varphi}(\zeta_k)$ and $h_k = \zeta_k - \zeta_{k-1}$.

To apply the scheme (4.4) to Eqs (4.3) we formulate them as the following set of first order differential equations

$$\frac{d\varphi_n}{d\zeta} = \sum_{m=1}^{8} a_{nm}\varphi_m + H_n \qquad n = 1, \ldots, 8 \tag{4.5}$$

where

$$\begin{aligned} &\varphi_1 = \overline{u} \qquad \varphi_2 = \frac{d\overline{u}}{d\zeta} \qquad \varphi_3 = \overline{v} \qquad \varphi_4 = \overline{p} \\ &\varphi_5 = \overline{T} \qquad \varphi_6 = \frac{d\overline{T}}{d\zeta} \qquad \varphi_7 = \overline{w} \qquad \varphi_8 = \frac{d\overline{w}}{d\zeta} \end{aligned} \tag{4.6}$$

From Eq (4.5) we have

$$\frac{d^2\varphi_n}{d\zeta^2} = \sum_{m=1}^{8}\left(\frac{da_{nm}}{d\zeta} + \sum_{l=1}^{8} a_{nl}a_{lm}\right)\varphi_m + \sum_{l=1}^{8} a_{nm}H_m + \frac{dH_n}{d\zeta} \tag{4.7}$$

Finally, for $n = 1, ..., 8$ we can write

$$\varphi_n^k - \frac{h_k}{2}\sum_{m=1}^{8} a_{nm}^k \varphi_m^k + \frac{h_k^2}{12}\sum_{m=1}^{8}\Big(\frac{da_{nm}^k}{d\zeta} + \sum_{l=1}^{8} a_{nl}^k a_{lm}^k\Big)\varphi_m^k +$$

$$-\Big[\varphi_n^{k-1} + \frac{h_k}{2}\sum_{m=1}^{8} a_{nm}^{k-1}\varphi_m^{k-1} + \frac{h_k^2}{12}\sum_{m=1}^{8}\Big(\frac{da_{nm}^{k-1}}{d\zeta} + \sum_{l=1}^{8} a_{nl}^{k-1}a_{lm}^{k-1}\Big)\varphi_m^{k-1}\Big] = \quad (4.8)$$

$$= \frac{h_k}{2}[H_n^k + H_n^{k-1}] - \frac{h_k^2}{12}\Big[\sum_{m=1}^{8} a_{nm}^k H_m^k + \frac{dH_n^k}{d\zeta} - \Big(\sum_{m=1}^{8} a_{nm}^{k-1}H_m^{k-1} + \frac{dH_n^{k-1}}{d\zeta}\Big)\Big]$$

Following Cebeci and Bradshaw (1984), the above system of equations with the boundary conditions can be written in the tridiagonal form

$$\hat{A}_k\varphi^{k-1} + \hat{B}_k\varphi^k + \hat{C}_k\varphi^{k+1} = \hat{H}_k \quad (4.9)$$

where $\hat{\mathbf{A}}, \hat{\mathbf{B}}, \hat{\mathbf{C}}$ are 8×8 complex matrices and $\hat{\boldsymbol{H}}$ is 8×1 matrix. The above system of equations is solved iteratively at every section; Newton's method is used to iterate on α so that the normalization condition (2.16) is satisfied. The algebraic system of equations is solved using the block elimination method.

5. Results

Calculations were made to test the non-parallel effect on the growth rate of disturbances. We analysed instability of flow around the 7 degree half-angle sharp cone of zero angle of attack at the free stream Mach number $\mathrm{Ma}_\infty = 8.0$ and $T_\infty = 53\,\mathrm{K}$. We compared the obtained results with experimental data of Stetson (1983), (1984) and numerical results of Dallmann (1993). These test cases were chosen because the only detailed stability experiment data available for a hypersonic flow (which is of primary interest here) were given by Stetson (1983), (1984) and Stetson and Kimmel (1992). The boundary layer edge Mach number and edge temperature of the experiment were equal to 6.8 and 70 K, respectively. Most of Stetson's data are growth rates $-\alpha_i$ versus disturbance frequencies F at a fixed Reynolds number. Comparison between the results obtained for $\mathrm{Re} = 1733$ using the local stability theory (for two different basic states) and the experimental data of Stetson is shown in Fig.5 and discussed in Section 2.

In Fig.6a, for the same test case, the amplification rates of second and first mode disturbances obtained from the local theory and parabolized stability theory are compared with the experimental data of Stetson. The instability

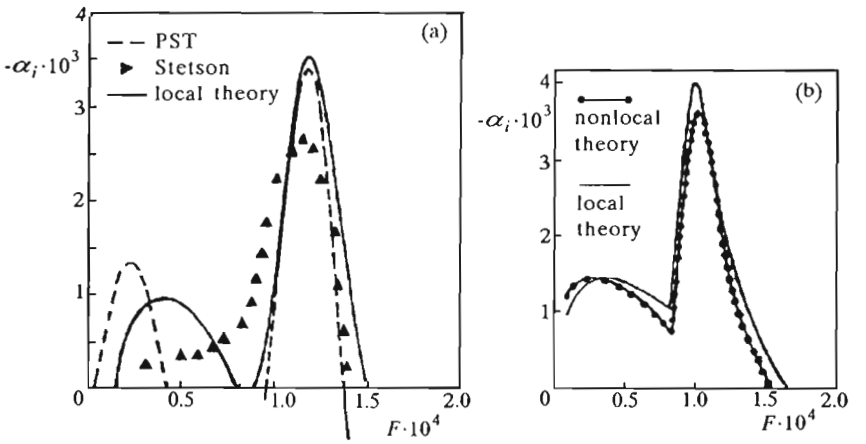

Fig. 6. Effect of nonparallelizm on the first and second mode characteristics; (a) – results obtained in present paper for the basic state from the thin layer Navier-Stokes equations, (b) – results obtained by Dallmann (1993) for similarity basic state

characteristics of first mode were obtained for $\gamma = 55$ degrees. All author's results analysed in this section were obtained for the basic state from the thin layer Navier-Stokes equations. The same comparision made by Dallmann (1993) is presented in Fig.6b. The instability characteristics showed in Fig.6b (Dallmann's results) were obtained for the basic state from the boundary layer equations. We see that nonparallelizm slightly stabilizes the second mode disturbances.

Fig.7 show the amplification rates of second mode disturbances obtained for the same geometry and freestream parameters as in Fig.6 but for different Reynolds numbers and for the frequencies $F = 126.0 \cdot 10^{-6}$, $F = 131.0 \cdot 10^{-6}$ using the local and parabolized theories. The same comparison made by Dallmann for $F = 73.4 \cdot 10^{-6}$ is shown in Fig.8. We can conclude that nonparallelizm slightly stabilizes the second mode disturbances for all the Reynolds numbers considered.

The nonparallel flow effect accounted for by the parabolized stability theory destabilizes the oblique first mode disturbances at lower Reynolds number and lower frequency and stabilizes at higher Reynolds numbers and higher frequencies. The influence of nonparallelizm on the first oblique disturbances is shown in Fig.9. In Fig.9 calculations were made for the wave angle $\gamma = 55$ and the frequencies: $F = 25.0 \cdot 10^{-6}$, $35.0 \cdot 10^{-6}$, $45.0 \cdot 10^{-6}$, $55.0 \cdot 10^{-6}$. The results obtained by Dallmann (1993) for $\gamma = 55$ and $F = 29.5 \cdot 10^{-6}$ are shown in Fig.10. From Fig.6 we see that a more complete stability analysis in-

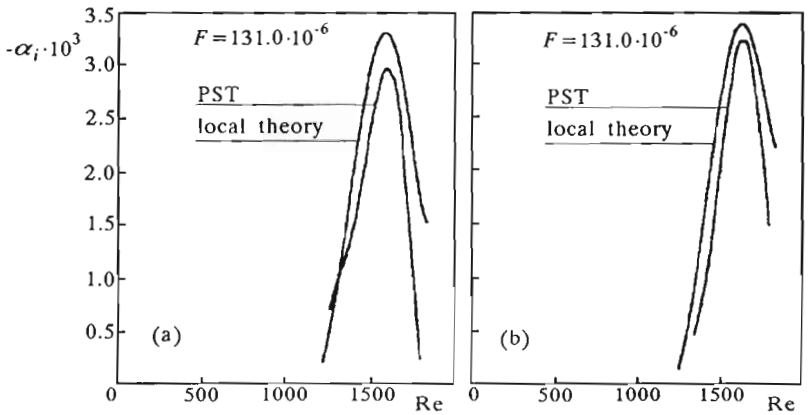

Fig. 7. Amplification rates of the second mode disturbances versus Re obtained from the local theory and parabolized theory for (a) $F = 131.0 \cdot 10^{-6}$ and (b) $F = 126.0 \cdot 10^{-6}$

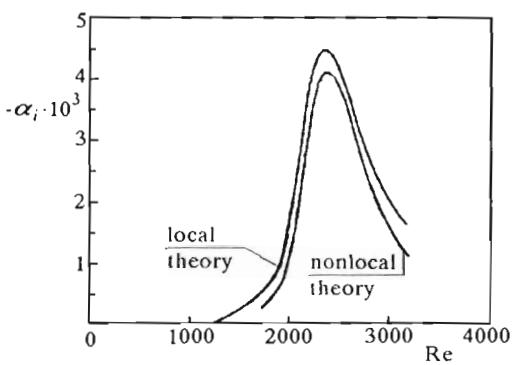

Fig. 8. Amplification rates of the second mode disturbances versus Re obtained from the local theory and parabolized theory for $F = 73.4 \cdot 10^{-6}$ by Dallmann (1993)

cluding non-local effects did not resolve the discrepancies between theory and experiment in the first mode region. According to Dallmann (1993) this can be explained by the fact that the conventional wind tunnel used by Stetson was "noisy" in the first mode region and in consequence the amplification rates obtained experimentally could be perturbed by the free stream disturbances.

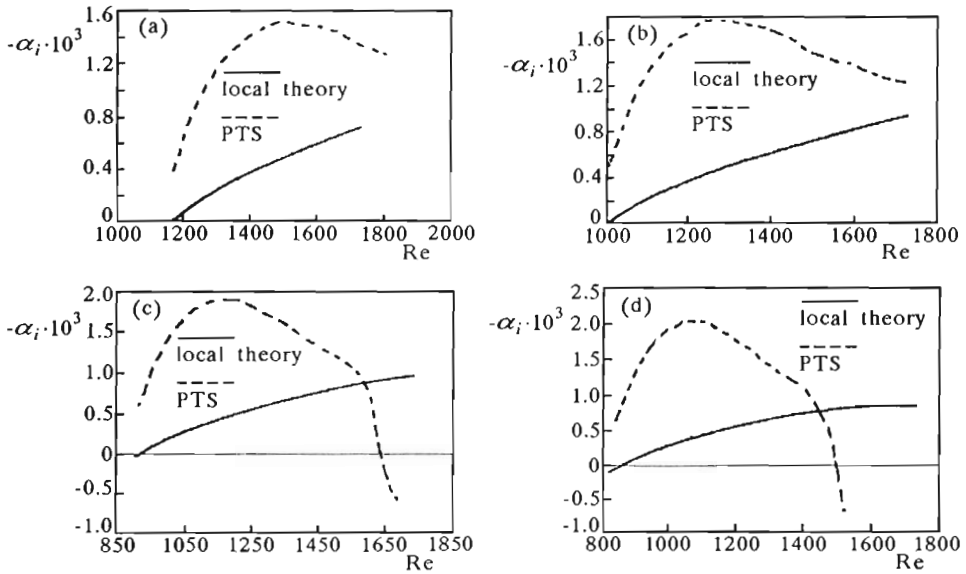

Fig. 9. Effect of nonparallelizm on the first mode characteristics for $\gamma = 55$ and for $F = 25.0 \cdot 10^{-6}$ (a), $F = 35.0 \cdot 10^{-6}$ (b), $F = 45.0 \cdot 10^{-6}$ (c), $F = 55.0 \cdot 10^{-6}$ (d)

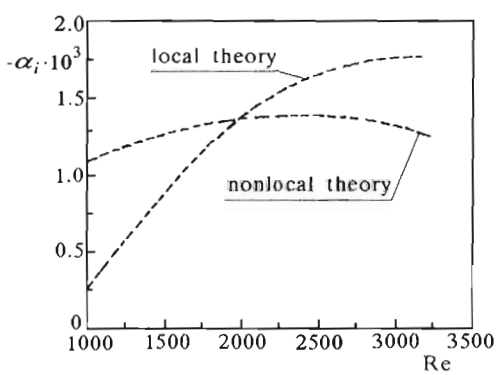

Fig. 10. Effect of nonparallelizm on the first mode characteristics for $\gamma = 55$ and for $F = 29.5 \cdot 10^{-6}$, Dallmann (1993)

6. Conclusions

In the present paper we analysed the influence of nonparallelizm on the instability characteristics of compressible flow around a sharp cone of zero angle of attack. A parabolized stability theory was introduced which describes the effects of nonparallel basic and disturbance flows on convectively unstable flows. We have found that nonparallelizm destabilizes the first mode disturbances at low Reynolds numbers and low frequencies and slightly stabilizes the second mode disturbances. For the second mode disturbances the agreement between experimental data of Stetson and theory is far better if viscous-inviscid interaction is taken into account.

The next issue to analyse is the influence of the bluntness of a body on instability of the boundary layer. The author plans to devote another paper to this problem.

Acknowledgment

The author is most grateful to Prof. Dipl.-Ing. Walter Riess from the University of Hannover for the great help during the scholarship visit and Dr U. Dallmann from DLR in Göttingen for remining accessible a highly accurate solution of the thin layer Navier-Stokes equations to perform the instability analysis.

References

1. BALACUMAR P., REED H., 1989, Stability of Three Dimensional Boundary Layers, Report of Department of Mechanical and Aerospace Engineering, Arizona State University
2. BERTOLOTTI F., 1991, Linear and Nonlinear Stability of Boundary Layers with Streamwise Varying Properties, Dissertation, Ohio State University, Columbus, USA
3. BERTOLOTTI F., HERBERT TH., SPALART P., 1992, Linear and Nonlinear Stability of the Blasius Boundary Layer, *J. Fluid Mech.*, **242**
4. CEBECI T., BRADSHAW P., 1984, *Physical and Computational Aspects of Convective Heat Transfer,* New York, Springer
5. CHANG C., MALIK M., HUSSAINI M., 1990, Effect of Shock on the Stability of Hypersonic Boundary Layer, *AIAA Paper,* 90-1448
6. CHANG C., MALIK M., ERLEBACHER G., HUSSAINI M., 1991, Compressible Stability of Growing Boundary Layers Using Parabolized Stability Equations, *AIAA Paper,* 91-1636
7. CHANG C., MALIK M., 1993, Non-Parallel Stability of Compressible Boundary Layers, *AIAA Paper,* 93-2912

8. DALLMANN U., 1993, Local and Nonlocal Instability of Hypersonic Flows, *Space Course,* TU München

9. EL-HADY N., 1981, On the Effect of Boundary Layer Growth on the Stability of Compressible Flows, *NASA CR-3474*

10. EL-HADY N., 1991, Nonparallel Instability of Supersonic and Hypersonic Boundary Layers, *Physic Fluids A.,* **3**, 9

11. GAPONOV S., 1981, The Influence of Flow Nonparallelizm on Disturbance Development in the Supersonic Boundary Layer, *Proc. of the 8th Canadian Congress of Appl. Mech.*

12. ILLINGWORTH C., 1953, The Laminar Boundary Layer of a Rotating Body of Revolution, *Philosophical Magazine,* **44**

13. MÜLLER B., 1991, Upwind Relaxation Method for Hypersonic Flow Simulation, *DLR-FB,* 91-36

14. SIMEN M., BERTOLOTTI S., HEIN S., HANIFI A., HENNINGSON D., DALLMANN U., 1994, Nonlocal and Nonlinear Instability Theory, *ECCOMAS, 2nd Computational Fluid Dynamics Conference,* Stuttgart

15. SIMEN M., DALLMANN U., 1992, On the Instability of Hypersonic Flow Past a Pointed Cone – Comparison of Theoretical and Experimental Results at Ma 8, *DLR-FB,* 92-02

16. STETSON K., 1983, Laminar Boundary Layer Stability Experiments on a Cone at Mach 8, Part I, *AIAA Paper,* 83-1761

17. STETSON K., 1984, Laminar Boundary Layer Stability Experiments on a Cone at Mach 8 Part II: Blunt cone, *AIAA Paper,* 84-0006

18. STETSON K., KIMMEL R., 1992, On Hypersonic Boundary Layer Stability, *AIAA Paper,* 92-0737

19. TULISZKA-SZNITKO E., 1993, *Niestabilność trójwymiarowej warstwy przyściennej,* Wydawn. Pol. Poznańskiej, 287

20. TULISZKA-SZNITKO E., 1996, Second Mode Instability, *Journal of Theoretical and Applied Mechanics,* **34**, 3, 641-661

Stabilność nierównoległych ściśliwych warstw przyściennych

Streszczenie

W pracy badana jest stabilność nierównoległej, ściśliwej warstwy przyściennej. Analizę przeprowadzono dla przepływu wokół stożka cylindrycznego o zerowym kącie natarcia i liczbie Macha przepływu niezaklóconego 8.0. Rozwój zaburzeń analizowany jest za pomocą parabolicznej teorii niestabilności oraz za pomocą teorii lokalnej. W pracy wyprowadzono równania parabolicznej teorii niestabilności dla przepływu wokół geometrii osiowosymetrycznej. Do dyskretyzacji równań w kierunku przepływu głównego zastosowano schemat wsteczny o dokładności drugiego rzędu natomiast w kierunku prostopadłym do powierzchni zastosowano schemat dwupunktowy o dokładności czwartego rzędu. W pracy badano wpływ uwzględnienia

nierównoległości przepływu na uzyskiwane charakterystyki pierwszych i drugich modów. Stwierdzono, że uwzględnienie nierównoległości przepływu nieznacznie stabilizuje drugi mod natomiast destabilizuje pierwszy mod dla małych liczb Reynoldsa i stabilizuje dla dużych liczb Reynoldsa. Stwierdzono, że bardziej precyzyjne zamodelowanie przepływu zaburzonego przez uwzględnienie nierównoległości przepływu nie wyjaśniło rozbieżności pomiędzy wynikami badań teoretycznych i eksperymentalnych w obszarze pierwszego modu.

Manuscript received March 20, 1996; accepted for print July 11, 1996